Ground Penetrating Radar Evaluation of Concrete Tunnel Linings

Graham Parkinson
Klohn Crippen Berger, 500-2955 Virtual Way, Vancouver, BC, V5M 4X6, Canada
e-mail: gparkinson@klohn.com

Csaba Ékes
Terraprobe Geoscience Corp., 4650 A Dawson Street, Burnaby, BC, V5C 4C3, Canada
e-mail : ekes@sfu.ca

Abstract - **Ground penetrating radar was used to map tunnel lining condition and locate concrete deterioration and voids in a continuous and non destructive manner. GPR surveying of Kapoor Water Supply Tunnel, Victoria, Canada was carried out with a 1000 MHz Sensors and Software Ltd., Conquest system mounted on a custom built cart. This 8.8 km long 2.3 m diameter concrete lined circular tunnel was surveyed in both directions in two days. During this time, major anomalies were drilled to verify interpretations of voids behind the liner. The 30 ns time window and 5 cm sampling interval used provided good data quality and allowed speedy data collection. The processed data provided a wealth of information on the condition of the tunnel lining. Five major types of anomalies were identified. These consisted of variations in water content, void spaces, embedded wood, faults and metallic objects. A guide to interpretation of these anomaly types is presented.**

The 17.58 km of GPR data taken in the tunnel showed that GPR continuously mapped concrete liner thickness, presence of reinforcement and delineated zones where mesh roof supports and construction support timbers are embedded in the liner, as well as the locations and orientations of faults that intersect the tunnel. Minor voids, honeycomb sections and areas of rock-liner separation were also detected. Radar responses to voids, zones of slight liner-rock separation, sharp rock pinnacles and hollows under the liner, and embedded wood all had slightly different characters, but were not always uniquely distinguishable from each other.

Keywords - **ground penetrating radar (GPR), tunnel inspection, concrete deterioration, tunnel engineering.**

I. INTRODUCTION

Tunnel inspections represent some near ideal circumstances for use of Ground Penetrating Radar and also some special challenges. The underground environment is one of the lowest electromagnetic background environments to work in and penetration can be excellent. The relatively constant geometry of concrete lined tunnels reduces clutter in the GPR images often caused by scattering from above ground objects. Operational challenges include internal multiple reflections within the tunnel that require appropriate filtering and the frequent requirement to image upwards which requires special apparatus to keep the antenna in contact with the tunnel roof. The degree of water saturation within the zone surrounding the tunnel may be variable, especially with tunnels that have been drained for inspection.

This paper describes a case history of a tunnel inspection within a concrete lined water supply tunnel conveying municipal water under gravity induced pressure. The tunnel passes under a mountain range and consequently has openings only at each end. As the main water supply to the nearby city of Victoria was interrupted by draining the tunnel, only a short amount of time was available to do the inspection which led to the requirement to conduct drill testing of the liner condition during the radar program instead of afterwards.

The Kapoor Tunnel is located in black slate schists, grey quartzose schists, and green chloritic (volcanic) schists. These rock types exhibit thin foliation and pronounced slaty cleavage or schistosity. Both the strata and schistosity are parallel and dip steeply to vertically.

The water supply tunnel was constructed in the 1960's and it was completed in 1970 using conventional drill and blast techniques, except for an initial problematic section excavated with a tunnel boring machine which was found to be unsuitable for the rock conditions encountered. The 2.3 m diameter, 8.8 km long tunnel has a circular section, except for the downstream 200 m, which is horseshoe shaped. The tunnel is concrete lined but it was not contact grouted during construction to fill voids and separations between the rock and liner which typically form at the crown (top) of the tunnel.

The tunnel was originally a free flow tunnel. To increase flow it was pressurized to a maximum design pressure of about 18 m. The purpose of the radar survey was to map discrete voids and crack, areas of separations of the concrete from the rock (defined as voids over scales greater than a metre with thicknesses less than 3 cm) and areas of poor quality concrete within the liner along survey lines in the crown area of the tunnel.

The drill and blast techniques used along the majority of the tunnel route typically result in rough rock surfaces. A 20 cm nominal thickness liner was poured over the rock to create a smooth inner surface using 24m long tubular forms filled with concrete by pumps. Unless extensive contact grouting is done, air trapped during construction and concrete shrinkage often results in construction voids around the irregularities of the rock, particularly in the crown area.

Erosional voids may also develop between the concrete liner and rock surface during service due to water flowing either in or out via construction joints or defects in the liner.

A previous radar survey of the tunnel condition conducted in 1991, used 500 MHz antennas. Areas of major voids identified in this survey were subsequently contact grouted, with several areas of substantial grout takes.

The 1000 MHz frequency of the Sensors and Software Noggin Conquest GPR unit used in the more recent survey were better suited to the conditions in the tunnel. The higher frequency was able to "see" more effectively between closely spaced steel reinforcements. The higher frequency also resulted in higher resolution of any void spaces within the lining. Data taken in the Kapoor Tunnel showed that the GPR continuously mapped liner thickness and quality, the presence of reinforcement and metallic roof supports, and locations where construction support timbers are embedded in the liner, as well as the locations and orientations of faults that intersect the tunnel.

Systematic interpretation of the 1000 MHz radar data independently produced a total of 401 anomalies, similar to the number of anomalies detected in the 500 MHz radar program, however areas that were previously contact grouted no longer showed void-like anomalies at the positions of previous voids, indicating that grouting efforts were generally successful in filling these voids.

Since complete records of tunnel construction are not available, the radar images are a valuable resource, with much interpretable information regarding construction methods, concrete character and geological details.

II. GPR SURVEY METHODOLOGY

Due to the length of the tunnel and the absence of any reference coordinate system, positioning accuracy became a key factor in following up the radar survey for testing or remediation work. As anomalies were often smaller in size than the cumulative error in positioning, it was necessary to mark anomalies in the field and to drill test these anomalies during the radar testing.

A continuous reading, rolling type of survey was performed using an 8 cm diameter odometer wheel attached to the antenna to trigger radar readings. Initially, a 1 cm reading interval and 40 ns time window was used for the readings but this was found to create unmanageable data volumes and problems with data integrity. The remainder of the survey was conducted with a 5 cm reading interval and a 30 ns time window, found to be better suited to the objectives of the survey.

A purpose built modular wooden push cart was designed with a counterbalanced antenna support arm mounted on a rotating head, to allow imaging along lines at any angle or directly overhead. The cart was designed with a pair of angled 40 cm pneumatic wheels to run along the lower haunches of the tunnel. A lower pair of wheels running along the tunnel invert supported two large lead acid batteries, one used for lighting and the other used for GPR power. The entire system had to be broken down into components smaller than 45 cm by 2 m to negotiate the access chambers provided for entry into the tunnel. The sketch below shows the basic design of this cart.

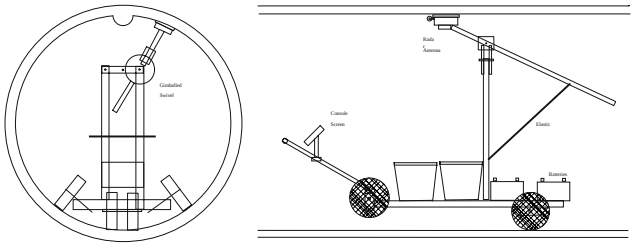

Before the survey commenced, a 50 cm diameter hand measure wheel run along the tunnel invert was used to stablish relatively accurate painted chainage marks on the tunnel wall at 100 m intervals. The GPR instrument odometer readings were logged and later corrected to agree with the more accurate measure wheel-based chainage marks. Based on the tie between a 1000 m wheel mark (measured downstream from the portal) and going back upstream 1000 m with the odometer, the corrected measurements were off by 9 m in closure when reaching the upstream portal after surveying upstream. The absolute location error was thus 9 m / 2000 m in this particular 2000 m loop or about 0.5%. Distance errors were attributed to roughness of the concrete ceiling of the tunnel affecting the small measure wheel on the antenna. Typical overall odometer location accuracy in the remainder of the tunnel sections is estimated to be about plus or minus 3-4 m or better.

The setup of the console and antenna on the cart was designed to allow the operator to observe both the antenna position and the screen on the console. Due to the small screen size of the console and limited visibility of a nomalies in the unprocessed raw data stream, not all anomalies could be marked as data were acquired. Marking all of the anomalies on the wall is not consistent with rates of forward progress required in such long tunnels, since identifying an anomaly and accurately marking the point required rolling the cart back. Anomalies are only evident on the screen against the background data once the cart has

passed the anomalous zone by several metres, making on-the-fly interpretation difficult. Major anomalies were noted in the field record and detailed by backtracking. Dragging a fixed tape would have instead allowed anomalies to be-marked on the fly. To aid in follow-up test drilling, positions were marked on the walls using chalk and wet marking spray paint normally used for timber grading marks and a field number / predetermined anomaly type marker code identifier was assigned.

To increase the signal to noise ratio, a data enhancing acquisition stack (cumulative average) of 2 pulse repetitions was used for each data point. In early tests, higher stack counts were evaluated, but noise was found to be sufficiently low due to the underground environment that a large number of stacks were not required, which allowed faster surveying.

Due to the normal antenna ringing and resolution limits, the optimum depth band for resolving detail in the 1000 MHz radar data taken through the partially saturated concrete liner was found to be in the 10 cm to 2 m depth range. This confirmed that the 1000 MHz is the optimum antenna frequency for mapping liner conditions in tunnels of this type. As is normal, antenna ringing is visible in the profiles as a series of bright bands at the beginning of the radar profiles. The waveform at this early part of the profile is mainly made up of the direct arrival of the airwave between antenna elements and artifacts from receiver settling.

Wavelengths of radar energy decrease while the wave slows as it enter the ground from the air. At 1000 MHz, the radar wavelength in air is approximately 30 cm. When the wave encounters wet concrete, the change in velocity results in a wavelength of about 10 cm.

Resolution of radar for objects within the concrete is dependent on wavelength and the size of the "footprint" caused by the radar's conical emission pattern from the antenna. The size of the footprint depends on depth, and was about 3 cm at the surface and about 15 cm at 1 meter depth for this system.

III. BASIC STANDARDIZED RADAR DATA PROCESSING

It was found best to prepare images using two processing streams. Raw, gain corrected images were produced using steps 1 to 4 and 7. Steps 1 to 9 were used to produce enhanced, migrated images. During interpretation both sets were compared.

1. Editing for data quality control and reposition traces to match chainage control points to correct for odometer errors.
2. Time zero corrections to flatten arrivals based on the direct wave.
3. Dewowing (removal of clipping and fluctuations in Rx amplitudes due to outgoing pulses).
4. SEC Gain: Gain started at 0.25 and used an exponential attenuation factor of 2.2 until limited to final gain of 500. The use of SEC gain with these parameters reduces early ringing and enhances deeper events, while preserving relative amplitudes useful for interpreting void bright spots.
5. Background subtraction. A horizontal filter was applied which subtracted a moving average of length 100 traces (5 m) from each trace. This effectively suppressed the banding artifacts caused by internal tunnel reflections.
6. Two-dimensional Migration. This filter used as input, the interpreted concrete velocity to geometrically collapse the hyperbolic arches to points. This reduced the visual interference of the rebar, simplifying the image, while also localizing the energy of anomalous areas, making the void anomalies stand out as a result of their increased amplitude.
7. Time to depth conversion: This was performed using a concrete velocity function established at 1.06 m/ns derived from analyses of diffraction hyperbola velocities at several locations. The numerous anomalies from reinforcements and rock pinnacles embedded in the concrete made this an effective method to determine concrete and rock velocities.
8. Blue-Grey-Red colour coding was applied to the filtered data, accentuating the higher amplitude anomalies, while suppressing anomalies in areas of more uniform concrete and in regions of good contact between the liner and rock.
9. Interpretation and overlay of interpreted concrete thickness (as a green line), identification of zones of concrete-rock separation, void spaces, honeycomb concrete condition layering and embedded wood features.

IV. GUIDE TO INTERPRETATION OF TUNNEL RADAR FEATURES

Radar profiles in the figures presented here are "upside down" relative to their actual orientations looking upward into the tunnel crown, since ground penetrating radar software customarily presents data looking downwards. The profiles have a depth scale in meters on the right axis, corresponding to about a 1 m total depth of investigation. The depth scale is derived from a picked average radar velocity in concrete of 1.06 m/ns.

In order to illustrate how voids and other features were identified, a "surface inwards" interpretation approach is used here to discuss features in the profiles consecutively inwards from the first event at the surface. Artifacts of the GPR method seen on the profiles, which are not related to subsurface features, are also discussed in the following section.

The dark high amplitude horizontal bands seen across the profiles, typically at multiples of 1.4 ns, are multiples of direct radar waves echoing across the air filled 2.3 m tunnel opening at the 3.33 m/ns air wave velocity. As tunnels are usually constant in width, this banding could best be filtered out to improve detail by using a tuned bandstop notch filter if available in software. This background was suppressed fairly effectively using a moving average background
subtraction filter which has a similar effect.

The disadvantage of a moving average background filter is that it also suppresses useful reflections that happen to be parallel to the tunnel face, such as those that occur primarily in tunnels driven by tunnel boring machine. For drill and blast tunnels, the rock contact is usually sufficiently variable to allow the use of moving average background subtraction to suppress tunnel multiples without loss of detail at the liner-rock interface.

IV.1 Identification of Concrete Honeycomb

Areas of honeycombed concrete (regions of bubble filled, poorly consolidated concrete) visible on the inner surface of the liner were observed to correspond to a distinct radar texture, as a result of the many small scattering centers. In the images these resulted in patterns of many small scale superimposed anomaly arches seen throughout the depth of the liner. Construction defect honeycombing or erosion of cement and exposed aggregate was often visible in the surface of the tunnel crown area, making it easy to correlate the GPR response to honeycombing in the concrete as the antenna passed over visible areas of it. An example of an area interpreted as honeycomb is outlined in blue on Figure 1.

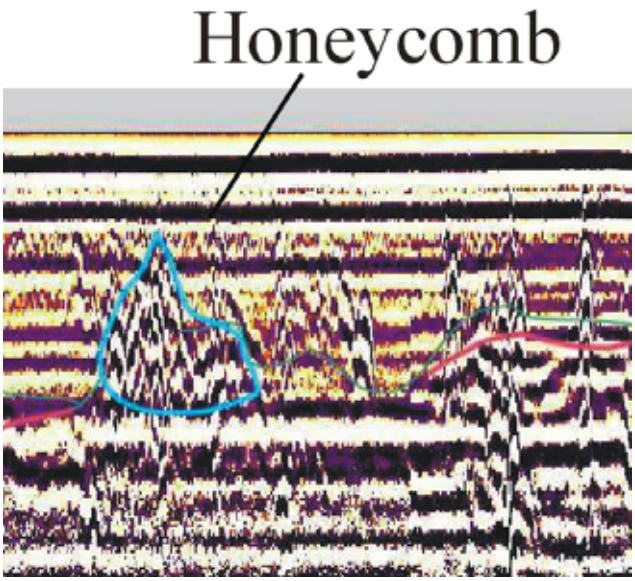

Figure 1. Anomaly type associated with regions of honeycombed concrete

IV.2 Identification of Reinforcement and Mesh Roof Support Sections

Regions of reinforcement were commonly encountered as illustrated in Figure 2. The narrow hyperbola with apexes near the surface are rebar or rock bolts within the concrete. The green line represents the liner – rock contact as interpreted from the migrated, background subtracted profile. The red line represents interpreted regions of one or two wavelength thick separation or void space between the liner and the rock. Due to the sufficiently high frequency of the 1000 MHz system regions between the rebar are well enough resolved to interpret regions of liner-rock separation behind the rebar section.

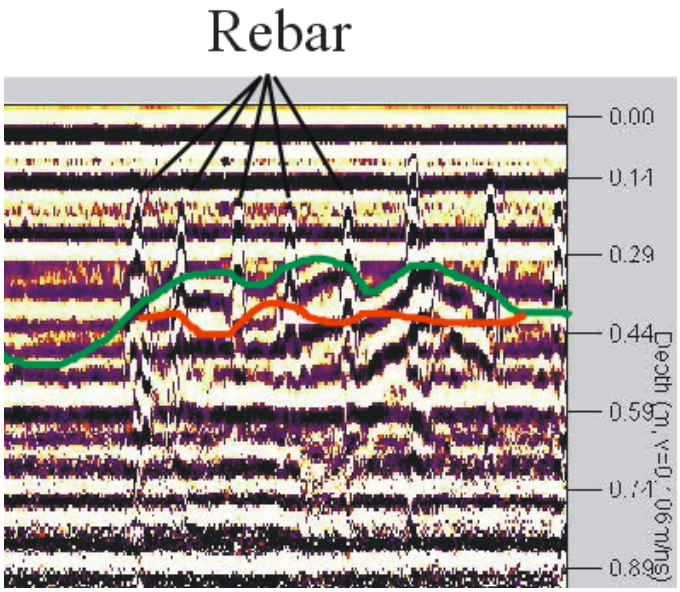

Figure 2. Section of tunnel with heavy density of rebar / roof support bolts.

IV.3 Identification of Embedded Square Set Wooden Timbers

Square set timbers produced a distinctive pattern of broad, high amplitude, coherent, parallel bands that were typically highly localized, showing sharp onset and ending abruptly. An example of a single timber embedded in the liner is marked in yellow on Figure 3. This is a raw, SEC gain corrected only image. Similar patterns in modeling of scattering by parallel faced objects by Daniels, 2004 [1] suggests that this type of anomaly is likely related to parallel faced timbers.

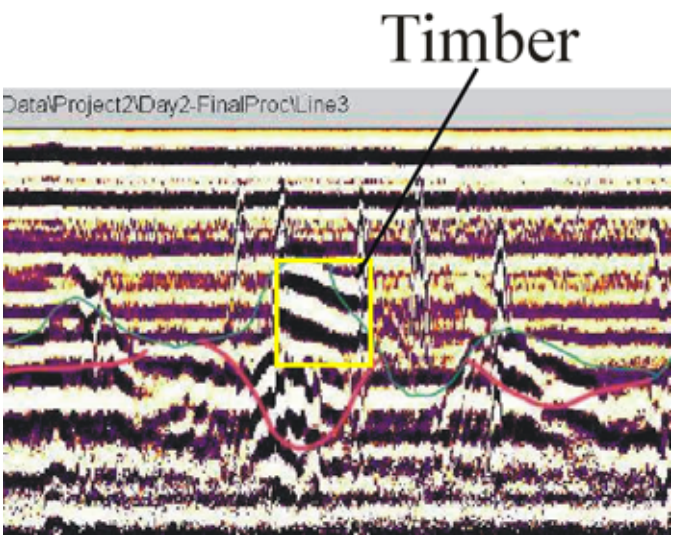

Figure 3. Anomaly characteristic of square set roof support timber

The hypothesis that this class of anomalies was related to wooden supports embedded in the concrete liner was tested by drilling several anomalies on the spot using a battery powered hammer drill. Holes were drilled with a 55 cm long 1 cm diameter bit. The cuttings were examined for evidence of material types and the walls of the holes were then probed with a bent wire to test for the thickness of any voids. After probing the holes, expanding pozzalanic grout was mixed in a dry pack and rammed into holes to seal drill holes. Figure 4 shows one of these anomalies and the location of a drill hole.

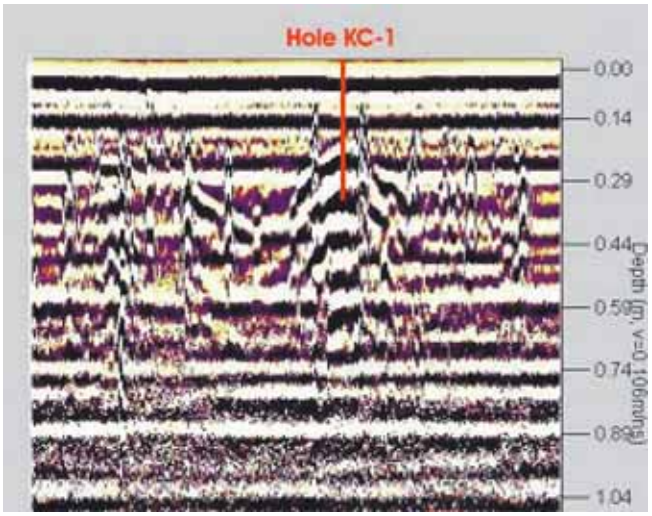

Figure 4. Drill hole test of timber anomaly

This 33 cm deep hole penetrated 13 cm of concrete liner material, 17 cm of wet wood, 5 cm of concrete and then went on into rock. This provided verification of the interpretation of wood being related to this type of anomaly.

The high amplitude of the timber anomalies is likely related to the parallel faces acting as good reflectors. Examples of groups of these anomalies are seen in Figure 5 and Figure 6.

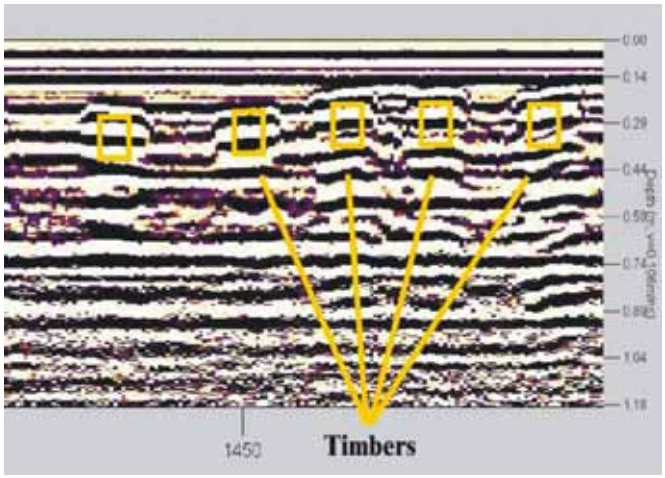

Figure 5. Group of square set timber anomalies

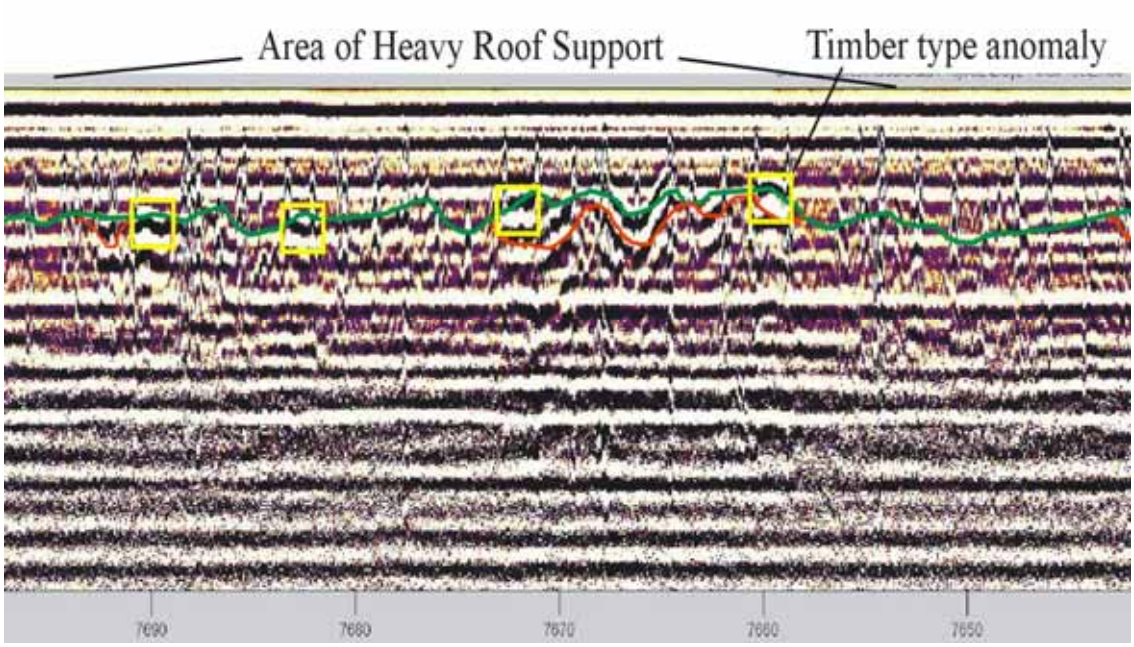

Figure 6. Region of heavy roof support

IV.4 Identification of Liner – Rock Contact

At the base of the concrete liner, a moderately well resolved and somewhat continuous reflection at the concrete-rock interface was usually seen, typically resolved as a doublet of paired black and white bands of irregular curvatures, connecting the apexes of the more prominent diffraction arches seen at rock pinnacles covered by the liner. This reflector was most interpretable on the SEC gained, background subtracted, migrated profiles. The interpreted liner-rock interface was marked in green on the example interpreted sections (Figure 7). It should be noted that the amplitude of the liner-rock reflection depends on the depth and curvature of the interface. Areas of thin concrete show stronger reflections at the base compared to deeper concrete liner sections.

IV.5 Identification of Voids at the Liner – Rock Contact

Areas of liner-rock separation or occurrences of thicker void spaces were sometimes seen along the concrete-rock interface. These zones are conspicuous by their pronounced irregular "bright spot" anomalies with higher amplitude and lower frequency (i.e. wider banding) relative to their surroundings. Areas of interpreted voids and separations are marked in red on the example interpreted sections.

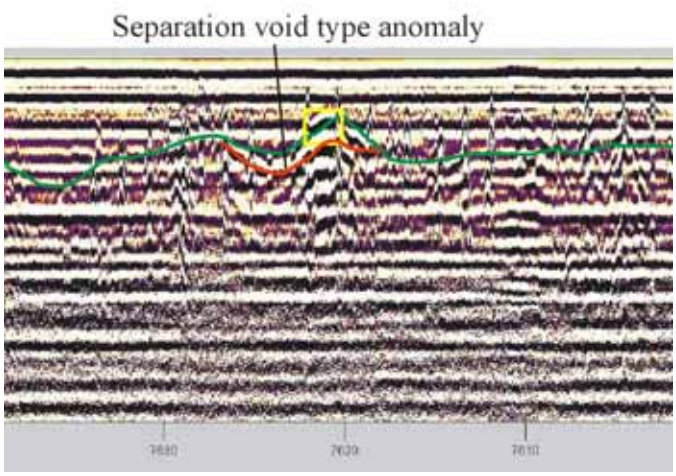

Figure 7. Liner-rock separation type anomaly

Voids were distinct from the similar amplitude and wavelength character anomalies over timbers due to a more gradual onset and larger extent of the regions of voids and separations. The voids tend to be found in concave regions of the tunnel roof as air becomes trapped in these regions during filling of the lining forms.

Separations of only several cm between the concrete and rock can result in changes to the "liner bottom reflector" character. Internal thicknesses of the void spaces are difficult to estimate as the bottoms of interpreted voids were rarely imaged directly. A void of more than a quarter wavelength in thickness (i.e. greater than about 2 cm to 3 cm in near saturated conditions) would be expected to

generate additional bands; however responses from the bottom of the voids were not separately identifiable.

IV.6 Features Seen Within the Rock Mass

The last events seen within the rock as the radar depth penetration fades into the characteristic "salt and pepper" noise background are typically patterns of cross cutting, deeper seated, diagonal limbs from diffraction arches. These are the remaining artifacts of radar energy scattering off of the rock features and pinnacles located closer to the concrete-rock interface. More distinct and diagonal features in this deep region correspond to reflections from fault planes in the rock. Figure 8 shows a diagonally cross cutting fault that also expressed itself as a series of small fractures in the surface of the concrete liner.

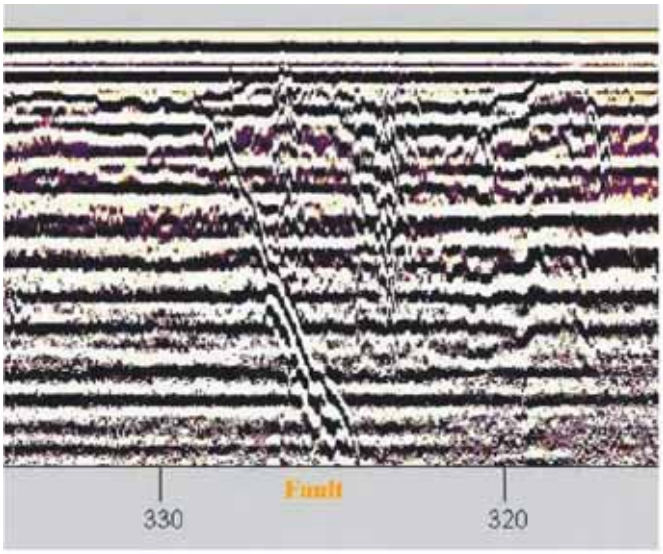

Figure 8. Fault crosscutting country wall rock

IV-1.Characteristics of the GPR Reflections from Voids and Effects of Data Processing

There are almost always more features visible in radar data than can be quickly accounted for by any simple system that classifies the anomalies of potential voids. Size, orientation, infill and depth to the void are all significant. This richness of information can be distracting and create a daunting task for the interpreter.

Data processing schemes and filters that accentuate the reflection at the concrete-rock interface are useful but may cause the signature of voids to become less prominent. An example of the effect of a 100-trace background filter is seen in Figure 11, "Background Subtraction Filtered Section". Conversely, filtering to enhance voids (e.g. Hilbert transform, migration etc.) may suppress the reflection at the intact concrete-rock interface.

For the purpose of this inspection, using both the unfiltered SEC gain presentation and the filtered background-migration filter data was found to be best for interpretation. An interpreter can often do best by comparing unfiltered data directly with filtered data to isolate particular feature types. The combined background and migration filter was particularly useful to highlight high amplitude anomalies of the types related to voids, separations and wood while suppressing background clutter.

V. GENERAL FEATURES INTERPRETABLE FROM THE RADAR IMAGES

Depths of features encountered in the drill holes placed to test anomalies were consistent with the depths interpreted from the radar images, suggesting that the concrete velocity of 1.06 m/ns determined from the fitting of hyperbolas to diffraction arches was accurate.

V-1.1 GPR Response Over Previously Contact Grouted Sections

Grouting had been completed at several sections that had been identified as suspected to contain excessive liner-rock void spaces, either from the results of the previous (1991) radar investigation or by "druminess testing" (testing for hollow sounds with a hand held hammer). During the present radar investigation these sections showed much lower densities of anomalies than surrounding sections of the tunnel. Figure 9 shows an example 1000 MHz profile from a contact grouted section. The almost featureless nature of the grouted section indicates that there are no voids between the liner and rock creating impedance contrasts sufficient to generate reflections or diffractions.

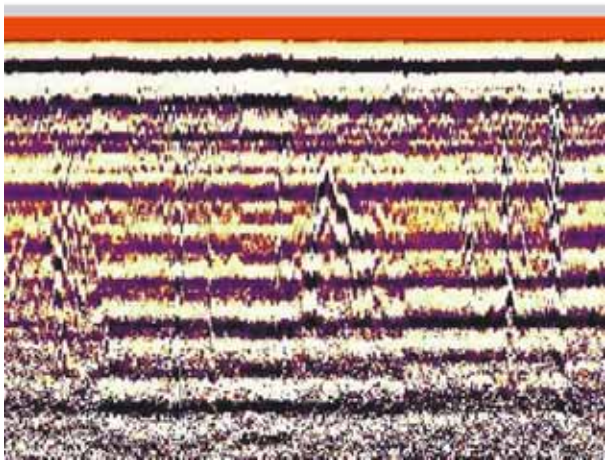

Figure 9. 1000 MHz GPR scan over previously grouted section

V-1.2 GPR Response Over End of Tunnel Boring Machine Section

Near the centre of Figure 10 at chainage 0+860 meters, the GPR profile clearly shows the location of the transition between the bored tunnel section and the drill and blast tunnel section. This is made evident by the transition seen between a relatively smooth and locally constant, 10 cm to 15 cm liner thickness in the initial, TBM section which was reported to be approximately 900 m long) and the locally

variable and overall much thicker concrete liner (averaging 25 cm to 30 cm) seen in the drill and blast section starting further downstream.

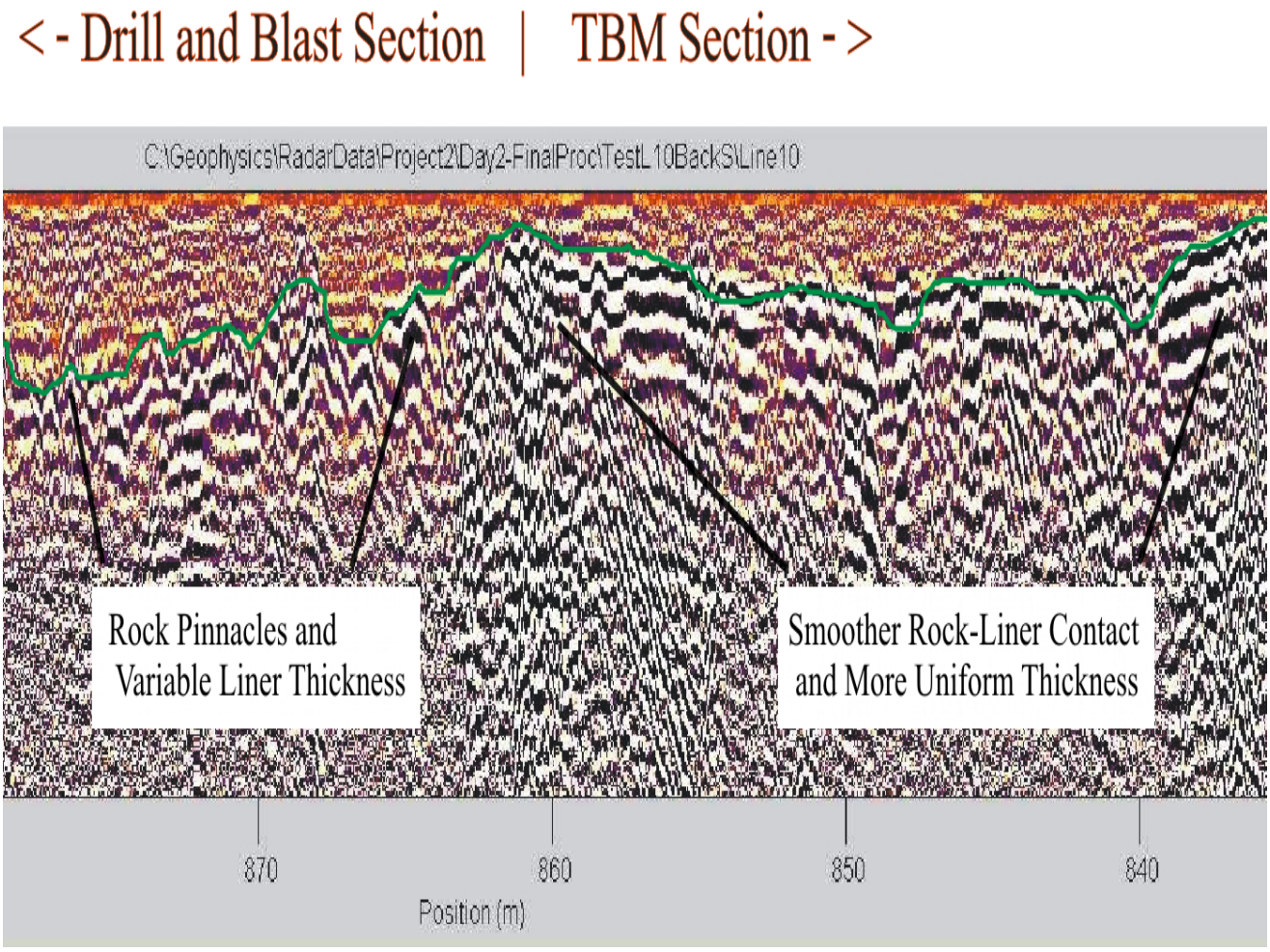

Figure 10. GPR profile over transition between TBM and drill-blast sections

In the TBM section of this profile, the undulating crown liner thickness on a scale of tens of meters appears to represent traces left in the rock of the tunnel by the reported tendency of the TBM to excavate down into the tunnel
invert in the soft rock. This problem likely led to the abandonment of the TBM method due to frequent downtime caused by the regular stops needed for jacking to realign the TBM.

V-1.3 Example of GPR Response at a Form Joint

In Figure 11, two profiles are presented, one above the other, showing different processing versions of the same section of tunnel data. The upper profile is a SEC gained, background subtracted, migrated version. This filtered profile presentation was used to interpret the green line marking the liner-rock contact. The lower profile is only SEC gained. This unfiltered profile presentation was used to interpret zones of separations and voids.

At chainage 4428m, near the right side of the profiles, a good example of a cold joint type liner anomaly can be seen. This was likely created at a formwork end between concrete pours. These types of anomalies that cut from surface to depth through the liner appear to be the result of water flows or retained water in the cracks and porosity of the circumferential cold joint.

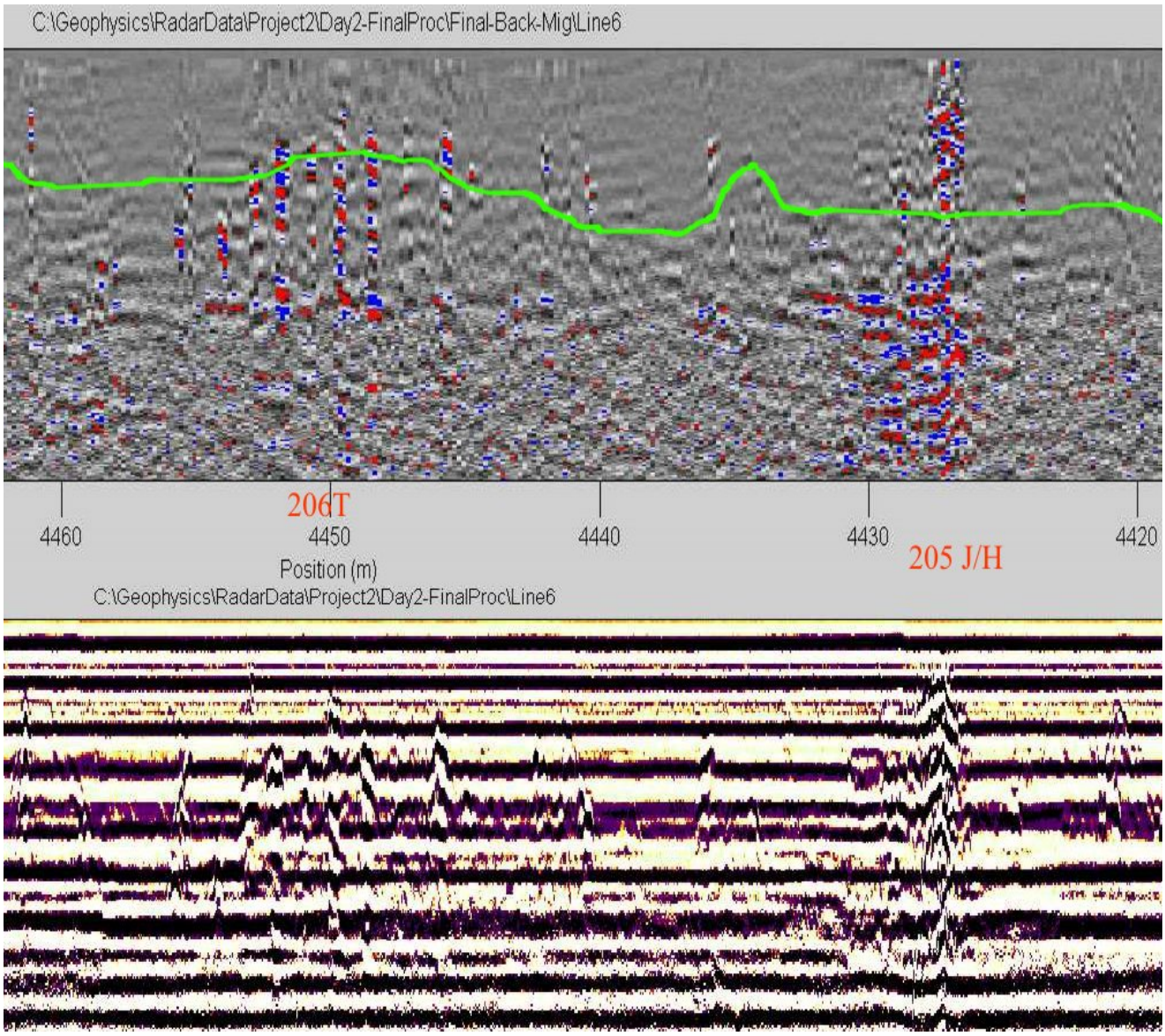

Figure 11. Migrated-Background Subtracted (top) and SEC Gained Profiles (bottom) over a Form Joint at 4428m

V-1.4 Results of Three Dimensional Detail Radar Grid Completed at 0+069

The ability of high frequency radar systems to automatically acquire 3 dimensional grid data cubes was used to detail an area of tunnel liner leaking water into the tunnel. This area was scanned in fine detail as a trial of using the radar in a handheld mode, following a preprinted grid panel on mylar. The greatest difficulty with this method was keeping the mylar panel attached overhead to the dripping wet tunnel wall as tape does not work in this situation. A small portable 12V vacuum pump and section of spaghetti tubing would have been useful to create suction to hold the mylar against the tunnel surface.

Images at various depths were sliced from the 30 depth planes and 13 horizontal and 13 vertical planes making up this data cube. Figure 12 shows one of these depth planes illustrating a horizontal feature found in the concrete liner (interpreted as probably resulting from an embedded wooden beam). The water inflow observed at this point (located at the intersection of planes G and 2) may have been passing through void space created by a rotting timber embedded in the liner. Alternatively, the concrete may have cracked around the perimeter of the timber, allowing water leakage.

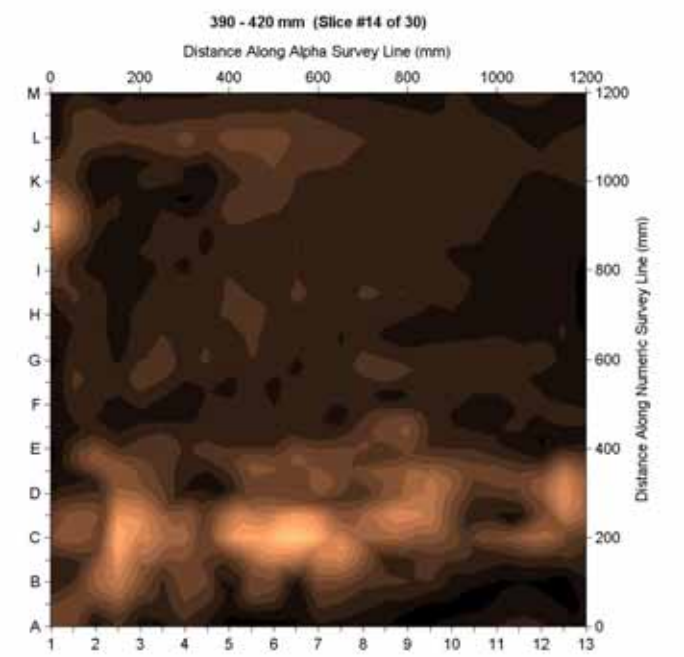

Figure 12. Depth plane image of horizontal embedded timber within leaking area of liner (Leakage at G-2)

V-1.5 Tabulations of Observed Anomalies and Use of Statistics on Anomaly Locations

Basing ongoing tunnel condition analyses on anomaly density between repeat surveys should be used with caution since visual identification of anomalies is a subjective process which can differ greatly between interpreters. It also depends on data presentation conditions (i.e. if done in the tunnel on a small screen with raw data or on a colour screen in an office, as well as the level of processing and filtering to enhance anomalies). The interpretation process is also difficult to standardize consistently across the large data sets representing the length of such a long tunnel.

The data processing, interpretation and presentation was simplified by breaking each of the two 8.8 km long lines into eighty-eight 100 m sections. Each section was presented in the two processing formats on an A3 sized sheet. Interpretation codes were then overlain on each section.

The system of labeling anomaly positions and identifier codes posted on the final sections used a two-part structure: i.e. "2H" indicates the second anomaly on the line, of honeycomb concrete type. In areas where features were superimposed, composite identifiers were used such as: 203 H/T i.e. anomaly number 203, interpreted as area of Honeycomb with Timber. The primary characteristic was listed first.

In total, 401 distinct radar anomalies were interpreted along the tunnel. Anomaly codes are presented in Table 1.

Table 1. Anomaly Identifier Codes

Identifier	Interpreted Anomaly Type	Number Interpreted (of primary type)*	Percentage
"V"	Void type	243	60.6%
"T"	Embedded timber	66	16.5%
"H"	Honeycombed concrete	52	13.0%
"F"	Fault or joint plane visible in rock beneath liner	16	4.0%
"J"	Poor quality (open) form joint	15	3.7%
"S"	Liner –rock separation	6	1.5%
"A"	Unspecified anomaly (steel etc.)	3	0.7%

* Total of unique interpreted anomalies was 401

VI. CONCLUSIONS

The 17.58 km of GPR data taken in the Kapoor Tunnel continuously mapped liner thickness, the presence of reinforcement and metallic roof supports, and locations where construction support timbers are embedded in the liner, as well as the locations and orientations of faults that intersect the tunnel. Voids, honeycomb sections and areas of rock-liner separation were also detected, tabulated as anomalies and located on transect plots of the tunnel. The numerous anomalies from rebar, rock bolts and steel roof supports were not included in the anomaly tabulations as they are distinctly separable from the void anomalies.

Based on analysis and drill testing of the features identified in the 1000 MHz survey (which had twice the resolution of the 500 MHz survey), it appears that many of the radar anomalies noted in the 1991 and in the current radar surveys are compact, high amplitude banded anomalies related to the wooden roof supports left in place when the concrete liner was poured. Timber and void anomalies can be quite similar.

Radar responses to discrete void spaces, zones of slight liner-rock separation, sharp rock pinnacles and rock hollows under the liner, and embedded wood all have slightly different characteristics. However, these types are not always uniquely distinguishable from each other as they were frequently coincident.

Other, more irregular separation type anomalies (seen as more extensive areas of high amplitude, sub-parallel nested sets of bands) are present at the liner – rock interface.

These appear to be related to gaps of several cm between the liner and rock.

The fine detail of the radar data offers the Tunnel Engineer a window on the construction and roof support methods used in the various sections, as well as a visual perspective on changes in the liner thickness and the character of the blasted rock surface. The radar also shows evidence of each individual rock bolt (which appears in the profiles below the liner) and reinforcing bar (which appears within the interpreted liner thickness).

Radar data needs to interpreted and classified or marked up by the geophysicist as the images are frequently too clutter ridden to be understandable by those unfamiliar with the method. Interpretation by the geophysicist to reduce the radar data to quantitatively defined zones of voids, zones of separation, and other anomalies and presentation in succinct tabulations or graphic overlays is important to create a record useful for engineering clients.

As complete construction records are no longer available, the radar images are a valuable resource, showing where areas of unstable ground where heavy roof supports were installed and geological details such as fault planes that intersect the tunnel. Engineering staff can make decisions based on the images to determine if zones of voids at the liner-rock contact significantly affect liner integrity, or are sufficiently bridged by intact concrete to not require remediation.

The program showed that repeat radar surveys performed before and after contact grouting can be used to establish the success of grouting programs designed to improve the seal between rock and concrete liner. Interpretation can be difficult but is possible with sufficient familiarity with the data and the inclusion of test drill holes placed in characteristic anomalies.

High frequency GPR data can be very feature-rich and fractal in nature. Interpretation of large data sets such as long tunnel transects can consequently be very time consuming. Contracts for tunnel inspections should include definite language as to the nature and scale of features for which interpretation is required. The use of a defined anomaly type table can simplify reporting and marking of anomaly types and locations in the field.

ACKNOWLEDGMENTS

Klohn Crippen Berger Ltd. and Terraprobe Geoscience Corp. wish to thank the staff of the Capital Regional Water District Water Department for their support during this program. We also acknowledge the patience of Garry Stevenson, P. Eng., and Project Manager, who graciously granted us just “a little more time”to“re-interpret a few more anomalies.

REFERENCES

[1] Daniels, D. J, Ground Penetrating Radar, 2nd Edition, 2004, IEE Radar, Sonar and Navigation Series, Institution of Electrical Engineers.

.